A hybrid strategy of offline adaptive planning and online image guidance for prostate cancer radiotherapy

2010 Phys. Med. Biol. 55 2221

(http://iopscience.iop.org/0031-9155/55/8/007)

Phys. Med. Biol. **55** (2010) 2221–2234 doi:10.1088/0031-9155/55/8/007

A hybrid strategy of offline adaptive planning and online image guidance for prostate cancer radiotherapy

Yu Lei[1,2] **and Qiuwen Wu**[2,3,4]

[1] Department of Radiation Oncology, Wayne State University, 4100 John R, Detroit, MI 48201, USA
[2] Department of Radiation Oncology, William Beaumont Hospital, 3601 West 13 Mile Rd, Royal Oak, MI 48073, USA
[3] Department of Radiation Oncology, Duke University Medical Center, Durham, NC 27710, USA

E-mail: Qiuwen.Wu@Duke.edu

Received 13 November 2009, in final form 17 February 2010
Published 30 March 2010
Online at stacks.iop.org/PMB/55/2221

Abstract

Offline adaptive radiotherapy (ART) has been used to effectively correct and compensate for prostate motion and reduce the required margin. The efficacy depends on the characteristics of the patient setup error and interfraction motion through the whole treatment; specifically, systematic errors are corrected and random errors are compensated for through the margins. In online image-guided radiation therapy (IGRT) of prostate cancer, the translational setup error and inter-fractional prostate motion are corrected through pre-treatment imaging and couch correction at each fraction. However, the rotation and deformation of the target are not corrected and only accounted for with margins in treatment planning. The purpose of this study was to investigate whether the offline ART strategy is necessary for an online IGRT protocol and to evaluate the benefit of the hybrid strategy. First, to investigate the rationale of the hybrid strategy, 592 cone-beam-computed tomography (CBCT) images taken before and after each fraction for an online IGRT protocol from 16 patients were analyzed. Specifically, the characteristics of prostate rotation were analyzed. It was found that there exist systematic inter-fractional prostate rotations, and they are patient specific. These rotations, if not corrected, are persistent through the treatment fraction, and rotations detected in early fractions are representative of those in later fractions. These findings suggest that the offline adaptive replanning strategy is beneficial to the online IGRT protocol with further margin reductions. Second, to quantitatively evaluate the benefit of the hybrid strategy, 412 repeated helical CT scans from 25 patients during the course of treatment were included in the replanning study. Both low-risk patients (LRP, clinical target volume, CTV = prostate) and intermediate-risk patients (IRP,

[4] Author to whom any correspondence should be addressed.

CTV = prostate + seminal vesicles) were included in the simulation. The contours of prostate and seminal vesicles were delineated on each CT. The benefit of margin reduction to compensate for both rotation and deformation in the hybrid strategy was evaluated geometrically. With the hybrid strategy, the planning margins can be reduced by 1.4 mm for LRP, and 2.0 mm for IRP, compared with the standard online IGRT only, to maintain the same 99% target volume coverage. The average relative reduction in planning target volume (PTV) based on the internal target volume (ITV) from PTV based on CTV is 19% for LRP, and 27% for IRP.

(Some figures in this article are in colour only in the electronic version)

1. Introduction

In external beam radiotherapy (EBRT) for prostate cancer, a major concern is the anatomical and positional variation of prostate and organ at risk (OAR), which often limits the accuracy of treatment, and thus reduces the efficacy of radiotherapy (de Crevoisier *et al* 2005, Heemsbergen *et al* 2007). This variation is mainly due to the setup error, i.e. inaccurate patient positioning and patient movement during the course of radiation therapy, and internal organ motion. Because nowadays the treatment plan is normally based on the treatment planning CT image, the setup error and internal organ motion can result in different delivered dose distribution from the planned one. This may produce insufficient dose coverage to the prostate tumor volume as prescribed and result in a decrease in tumor control rate (Bos *et al* 2005). On the other hand, if the OAR is not at the same position as in the planning CT image, it may potentially get over-dosed and develop high levels of complications (Zelefsky *et al* 2002, Koper *et al* 2004).

The setup error correction in prostate radiotherapy has been covered by many studies. The setup error can be measured by comparing the MV portal images obtained by an electronic portal-imaging device (EPID) with reference to a simulation film or digital reconstructed radiograph (DRR) based on a bony structure (Wong *et al* 1995, de Boer and Heijmen 2001, Herman *et al* 2001, Ghilezan *et al* 2005). Both online and offline strategies have been proposed and implemented to correct setup error (Wu *et al* 2006). The online correction is defined as adjusting the patient and beam position at each treatment fraction, while the offline correction involves determining and adjusting the patient position based on the accumulated information from the early finished treatment fractions. In principle, the offline correction can significantly reduce the setup error (Bel *et al* 1996, Yan *et al* 2000, Amer *et al* 2001, de Boer and Heijmen 2001), especially the systematic component. However, the random components can only be compensated in the treatment margins. In contrast, the online correction can correct and eliminate both the systematic and random setup errors, but it may extend the treatment time considerably (Van de Steene *et al* 1998, Stroom *et al* 2000), and therefore may not be practical for regular fractionated treatment. In addition, the rotations are not usually corrected due to limitations of the linear accelerator patient positioning system (i.e. treatment couch).

In contrast, the management of uncertainties caused by prostate motion is more challenging. The shape and position of prostate and seminal vesicles (SVs) are affected mostly by the physiological change of rectum filling and, to a lesser degree, by the change of bladder filling (Ten Haken *et al* 1991, Balter *et al* 1995b, Roeske *et al* 1995), and both the intra-fraction and inter-fraction organ motion and deformation can have a significant impact

on treatment delivery if they are not accounted for. In offline adaptive radiotherapy protocol (ART), the inter-fraction organ motion, including rotations and deformations, is accounted for by constructing a patient-specific planning target volume (PTV) from clinical target volumes (CTV) from a few early fractions (Yan *et al* 2000). For online image guidance, radio-opaque fiducial markers implanted in the prostate gland are commonly used (Balter *et al* 1995a, Millender *et al* 2004). Similar to the setup error correction, online image guidance (IGRT) can only correct for the translational motions of the CTV. The rotation and deformation cannot be corrected and they are only accounted for during the treatment planning through the use of margins.

The offline and online IGRT for prostate have their own advantages and disadvantages. The aim of this work was to propose a hybrid strategy of online image guidance and offline adaptive treatment planning for prostate cancer radiotherapy. The rationale of the necessity of offline adaptive planning in online image-guided radiotherapy was studied first, and then the new hybrid strategy was proposed and simulated, and its benefit in margin reduction was evaluated geometrically.

2. Materials and methods

2.1. Is offline adaptive planning necessary for online image-guided radiotherapy of prostate cancer?

The inter-fraction prostate motion includes the rigid motion (translation and rotation) and non-rigid motion (deformation) with respect to the planning CT. In online image-guided radiotherapy, the inter-fractional prostate translational motion was corrected by couch shift, the rotational motion and organ deformation are not corrected and additional margins are applied in treatment planning. In offline ART, both the rigid and non-rigid motion/setup error can be included. However, only the systematic component can be corrected, the random component cannot be corrected but can be accounted for by using proper margins in the ART planning. Therefore, the efficacy depends on the motion characteristics. In this part of the study, we investigated the characteristics of the residual prostate motion for an online image-guided protocol. Specifically, the prostate rotation was analyzed.

A total of 592 cone-beam computed tomography (CBCT) images from 16 prostate cancer patients who underwent an online image-guided hypo-fractionated protocol were included in this part of the study. These CBCTs were taken either before (pre-CBCT) and/or after (post-CBCT) each treatment fraction. Each patient has three gold coils (Visicoil, IBA, Bartlett TN) implanted in the prostate gland. All CBCT images were registered to the planning CT based on the Visicoil locations, and translational correction was performed based on the registration of pre-CBCT at each fraction. Only rigid translation was performed because the correction can only be made by a couch shift. The relative displacements (dX, dY, dZ) and rotations (rX, rY, rZ) in pre- and post-CBCTs with respect to the planning CT were measured by the six degree-of-freedom (DOF) registration between CBCT images and planning CT image. The X, Y and Z axes are defined as the left–right, superior–inferior and anterior–posterior directions with positive value indicating left, anterior and superior directions, respectively. The rotations (rX, rY, rZ) are along the (X, Y, Z) directions with positive values in the right-hand-rule direction along the axis of rotation.

The following statistical analyses were performed based on these data.

(1) The mean and standard deviation of (rX, rY, rZ) from pre-CBCT were calculated for each patient, and Student's t-test was applied to evaluate whether the inter-fractional systematic

component is significantly different from 0; the patient specificity was tested by ANOVA on all 16 patients in each of those three directions.

(2) The correlations between rotations of pre- and post- CBCT were measured by the Pearson's correlation coefficients (R^2).

(3) The representativeness of the rotations in the first five fraction treatments for those in the subsequent fractions was studied by comparing their variances (Levene's test) and means (Welch's t-test) in pre- and post-CBCTs.

The deformation was not studied in this part because the CBCT image does not have adequate quality for delineating the prostate gland accurately.

2.2. Geometric evaluation of hybrid strategy of online and offline image guidance

In the hybrid strategy that we propose, a patient is treated with online image guidance in which the patient position is corrected through couch shift based on pre-CBCT scans. After a few (5) treatment fractions, a new modified plan will be generated based on the measured residual motions and deformations. The benefit of this hybrid strategy over the standard online correction protocol is evaluated in the following simulation.

For this part of the study, repeated helical CT images of the pelvic region from 25 patients over 412 fractions previously treated under the in-house ART protocol were used. Twenty-three patients had at least 15 treatment CT scans, sampled with 3 mm slice thickness. For each CT image, the contours for prostate and seminal vesicles (SVs) were delineated by experienced planners. The treatments for both low and intermediate-risk prostate cancer patients were investigated. The difference is in the CTV definition, where for low-risk patients (LRP) the CTV is equal to the prostate gland, and for intermediate-risk patients (IRP), the CTV is the combination of prostate gland and SVs. Since the CTV contours were used, both rotation and deformation effect were included in this part of the study.

2.2.1. Online image guidance. The online image guidance was simulated as a translation of the center-of-mass (COM) of the CTV. The thickness of the helical CT slices of CT images was 3 mm, whereas the magnitude of online correction could be smaller than 3 mm. To avoid the round-off error by the CT slice thickness (the axial CT image already has the resolution of smaller than 1 mm $\times$ 1 mm.), the original CT images and contours were interpolated into 1 mm thick slices. Let CT_1 and CT_2 be the CT numbers of two contiguous pixels of two adjacent slices; the CT values of interpolated pixel were then calculated by the weighted arithmetic average, i.e. $CT_{i,1} = (2 \times CT_1 + CT_2)/3$, and $CT_{i,2} = (CT_1 + 2 \times CT_2)/3$, where $CT_{i,1}$ is the CT value of the pixel closer to the pixel with CT value CT_1, and $CT_{i,2}$ to CT_2 (figure 1). The contours delineated on the images were accordingly interpolated by Pinnacle^3 planning system (Philips Radiation Oncology Systems, Fitchburg, WI). All of the following study was based on these interpolated images and contours.

To simulate the online image-guided correction, the planning CT was used as a reference, and the coordinates of COM of CTV in both planning CT and treatment CTs were calculated in the Pinnacle^3 System. Let $(x_r, y_r, z_r)_{COM}$ be the coordinates of COM of CTV in reference CT, and $(x_t, y_t, z_t)_{COM}$ be the COM of CTV in treatment CT. The difference $(\Delta x, \Delta y, \Delta z) = (x_r - x_t, y_r - y_t, z_r - z_t)_{COM}$ was calculated and the corresponding treatment CTs were shifted with the vector $(\Delta x, \Delta y, \Delta z)$, as demonstrated in figure 2.

After the online correction, the translational components in setup error and organ motion were assumed to be removed.

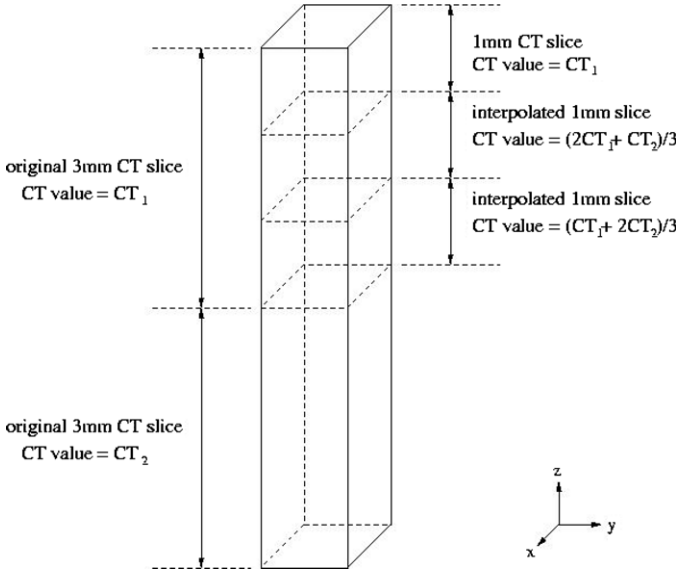

Figure 1. A regular 3 mm helical CT scan is interpolated into 1 mm slice thickness to improve the simulation accuracy of online image guidance.

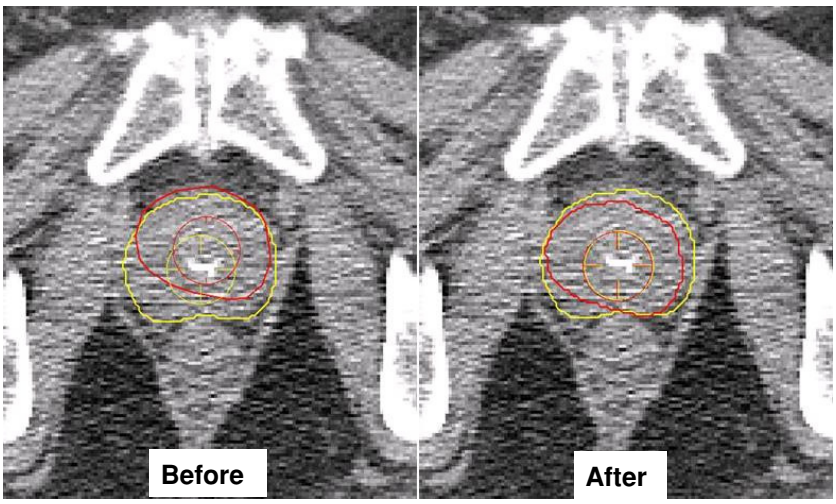

Figure 2. Simulation of online image guidance on one axial CT slice. The center of the yellow circle is the COM of the prostate (yellow contour) in reference CT. The prostate and its COM on treatment CT are in red. Before online correction (left), after online correction based on COM (right).

2.2.2. Offline image guidance strategy and ITV design. The offline image-guided adaptive radiation therapy typically uses the information from post-treatment images (residuals) from a few early treatment fractions to modify the treatment plan for subsequent treatment delivery. In our simulation, the new internal target volume (ITV_n) for prostate and for prostate plus SVs was constructed based on the treatment images of the first five treatment fractions.

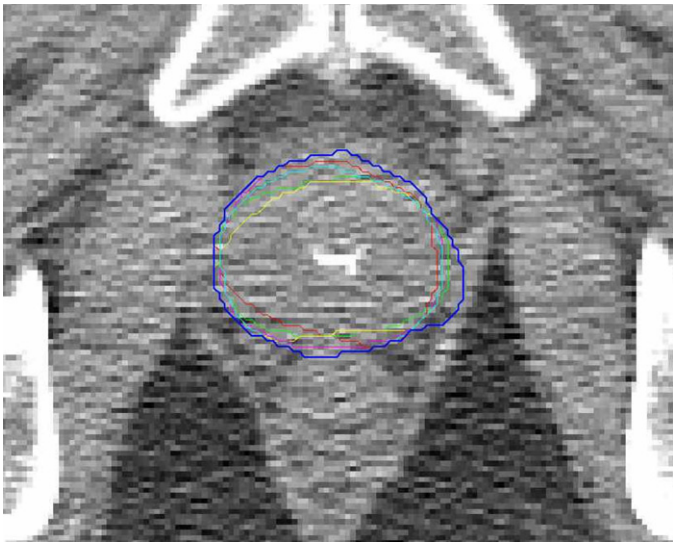

Figure 3. Forming of ITV_n from the CTVs on an axial CT slice. Yellow, red, green, light blue are CTV_i in treatment CTs after online correction. Dark blue is the ITV_n, which is the composite of others.

The ITV_n was constructed after the online correction through which the rigid translational components of the setup error and inter-fractional organ motion have been removed. Let CTV_0 be the CTV from planning CT of a patient; the CTVs from treatment CTs be noted as CTV_i, $i = 1, 2, \ldots, N_f$, where N_f is the total number of treatment fractions. The ITV_n is defined as the union of the online corrected CTV_i from the first five treatment CT images, i.e.

$$ITV_n = \bigcup_{i=1}^{5} TM_i[CTV_i], \tag{1}$$

where TM_i is the translational transformation matrix used in online correction; CTV_i is CTV at the ith treatment fraction. An example of the construction of ITV_n in transverse view is shown in figure 3. We want to point out that here the ITV_n does not include the CTV_0, as was done in standard offline ART. This is to remove any possible systematic differences between simulation and treatment. The ITV_n will then be used in replanning for the subsequent treatment fractions.

2.2.3. Geometric evaluation. The evaluation of the image-guided adaptive radiotherapy strategy can be done geometrically and/or dosimetrically. In this study, the geometric evaluation of the hybrid strategy is performed.

The volume overlap index (OI) is utilized for geometric evaluation. For ITV_n, the volume overlap index in the ith treatment fraction (OI_i) is defined as the fraction of online corrected CTV_i volume that intersects with the volume of margin added ITV_n, i.e.

$$OI_i(ITV_n + M) = \frac{\text{Volume}((ITV_n + M) \cap TM_i[CTV_i])}{\text{Volume}(CTV_i)}, \qquad (i = 6, 7, \ldots, N_f). \tag{2}$$

Here ITV_n is defined as in (equation (1)); M is the uniform margin added to ITV_n, and a range of 0–10 mm was evaluated here; CTV_i is the CTV at the ith treatment fraction; TM_i

is the translational transformation matrix used in online rigid correction; N_f denotes the total number of treatment fractions. The operator $\cap$ defines the common volume between two regions of interest. The OI_i ranges from 0 to 1, and the larger the OI_i, the better the ($\mathrm{ITV}_n + M$) covers the CTV_i. Similarly, for CTV_0, OI_i is defined as

$$\mathrm{OI}_i(\mathrm{CTV}_0 + M) = \frac{\mathrm{Volume}((\mathrm{CTV}_0 + M) \cap \mathrm{TM}_i[\mathrm{CTV}_i])}{\mathrm{Volume}(\mathrm{CTV}_i)}, \qquad (i = 6, 7, \ldots, N_f). \tag{3}$$

The benefit of ITV_n can be evaluated by comparing the volume of margin added ITV_n (i.e. $\mathrm{Vol}(\mathrm{ITV}_n + M)$) with the volume of margin added CTV_0 (i.e. $\mathrm{Vol}(\mathrm{CTV}_0 + M)$) when they have equal OI_i. The smaller $\mathrm{Vol}(\mathrm{ITV}_n + M)$ means better geometric coverage of ITV_n than CTV_0. In other words, we can examine the difference between their required margins for ITV_n and CTV_0 to achieve the same OI_i. Only the uniform margin was evaluated in this study.

In order to fairly compare the volume of margin added CTV_0 and ITV_n, the initial volume difference between ITV_n and CTV_0 should be considered. Inherently, as the union of the first few fraction treatment CTVs, ITV_n should have a larger volume than CTV_0. It is equivalent to the volume of CTV_0 plus a certain amount of uniform margin, say, M_0, i.e. $\mathrm{Vol}(\mathrm{CTV}_0 + M_0) = \mathrm{Vol}(\mathrm{ITV}_n)$. If the margins for CTV_0 and ITV_n corresponding to a certain OI_i are $M_{C,\mathrm{OI}i}$ and $M_{I,\mathrm{OI}i}$, i.e. $\mathrm{OI}_i(\mathrm{CTV}_0 + M_{C,\mathrm{OI}i}) = \mathrm{OI}_i(\mathrm{ITV}_n + M_{I,\mathrm{OI}i})$, the equivalent margin difference ΔM can be defined as the difference between $M_{C,\mathrm{OI}i}$ and $M_{I,\mathrm{OI}i}$, after subtracting M_0, i.e.

$$\Delta M = M_{C,\mathrm{OI}i} - M_{I,\mathrm{OI}i} - M_0. \tag{4}$$

This equivalent margin difference ΔM is used as a fair measure of the benefit of ITV_n over CTV_0. A larger ΔM implies a better geometric coverage of ITV_n than that of CTV_0 for the target volume. When the volumes of CTV_0 and ITV_n with different margin added are given, the relationship between margins added target volume and the margin can be obtained by fitting with a quadratic function. Then M_0 is calculated from the fitted target volume–margin relation and the volumes of CTV_0 and ITV_n. Similarly, the relation between OI_i and margin is fitted, and the corresponding margins ($M_{C,\mathrm{OI}i}$ and $M_{I,\mathrm{OI}i}$) to the OI_i are interpolated from the fitted functions. With M_0, $M_{C,\mathrm{OIi}}$ and $M_{I,\mathrm{OIi}}$ obtained, the equivalent margin difference ΔM can then be calculated.

3. Results

3.1. Rationale for offline adaptive planning

The mean and standard deviation of rX, rY and rZ from pre-CBCTs were calculated for each patient. The inter-fractional systematic component of rotation was measured by the mean value (i.e. $\langle \mathrm{r}X \rangle$, $\langle \mathrm{r}Y \rangle$ and $\langle \mathrm{r}Z \rangle$), and Student's t-test was applied to test the significance of the systematic rotation. There were 10, 10 and 11 out of 16 patients who have $\langle \mathrm{r}X \rangle$, $\langle \mathrm{r}Y \rangle$ and $\langle \mathrm{r}Z \rangle$ significantly different from 0° ($p < 0.05$) respectively, as shown in figure 4.

The patient specificity of the inter-fractional component of rotation was tested by ANOVA. If the resulting p-value is smaller than 0.05, the rotation is thought to be patient specific. For $\langle \mathrm{r}X \rangle$, $\langle \mathrm{r}Y \rangle$ and $\langle \mathrm{r}Z \rangle$, the p-values of ANOVA test are 0.000 23, 0.027 and 0.43, respectively; therefore, these rotations are at least patient specific in $\langle \mathrm{r}X \rangle$ and $\langle \mathrm{r}Y \rangle$ axes.

As a measure of the persistence of the inter-fractional component of rotation throughout each treatment fraction, the correlations between rotations of pre- and post-CBCT in three directions were investigated respectively and measured by the square of Pearson's correlation coefficients (R^2). Rotations with magnitude smaller than 1.5° were excluded from this analysis since only the persistence of large internal organ rotation is of importance. Strong associations between rotations in pre- and post-CBCT images were observed for rX ($R^2 = 0.77$), and rZ

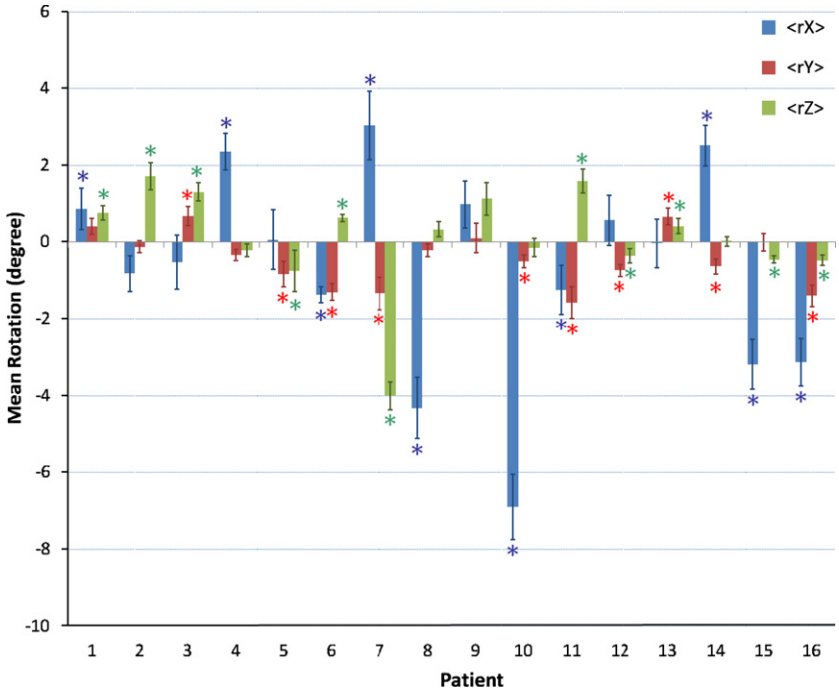

Figure 4. Mean rotations between treatment CBCTs and planning CT in X, Y and Z directions for all 16 patients. Error bar is one standard deviation. Bar with '*' means that the mean value is significantly different from zero (t-test $p < 0.05$)

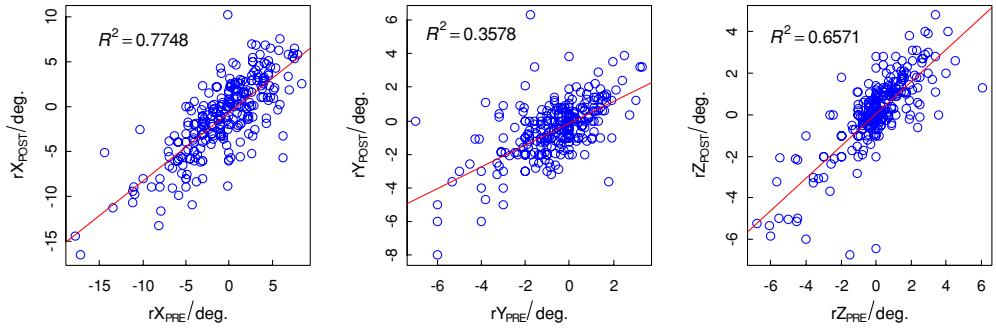

Figure 5. Correlations between rotations in pre- and post-CBCTs. R^2 are calculated from linear regression from rotations with magnitude larger than 1.5 degree.

($R^2 = 0.66$), and a bit lower for rY ($R^2 = 0.36$), as shown in figure 5. This indicates that if a large rotation exists before the treatment fraction, it likely remains during the treatment, and therefore the intra-fractional rotation is relatively smaller than the inter-fractional rotations.

The representativeness of the rotations in the first 5 days treatments for those in the subsequent fractions was studied by comparing their variances and means in pre- and post-CBCTs. Levene's test was used to compare the variances. Welch's t-test was used to test if

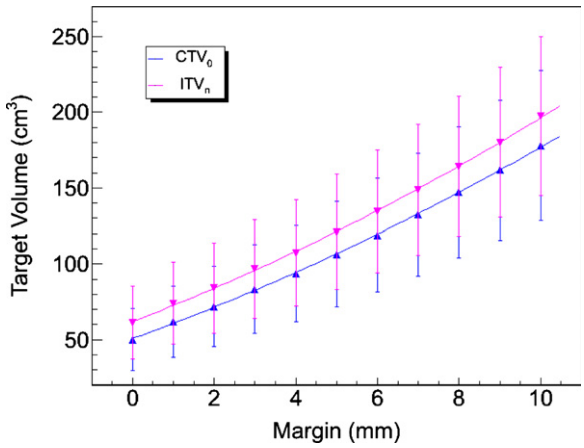

Figure 6. The relation between absolute target volume of CTV_0 and ITV_n versus margin for low-risk patients. The lines are fitted quadratic functions.

Table 1. Numbers of patients with equivalent means and variances of the rotations in X, Y and Z directions between the first five and the remaining fractions. The total number of patients is 16. $\langle . \rangle$ = mean value, VAR(.) = Variance, PRE = CBCT data taken before the treatment, POST = CBCT data taken after treatment. Levene's test is used to test the equality of variances, and Welch's t-test to test the equality of means. If $p > 0.05$, we accept the null hypothesis that the quantities tested are equal.

Data type	$\langle rX \rangle$	$\langle rY \rangle$	$\langle rZ \rangle$	VAR(rX)	VAR(rY)	VAR(rZ)
PRE	11	13	13	13	13	13
POST	14	11	13	16	15	12

the mean of the first five fractions of data is significantly different from that of the remaining treatment fractions. Table 1 shows that for both pre- and post-CBCT images, for the majority of patients studied, the means and variances of rX, rY and rZ of the first 5 days are equivalent to those of the subsequent treatment fractions.

3.2. Geometric evaluation of the hybrid strategy of online and offline image guidance

The relations between margin and patient average target volume for ($CTV_0 + M$) and ($ITV_n + M$) are shown in figure 6 for both low- and intermediate-risk prostate cancer patients. Without any margin added, as expected, the average volume of ITV_n over all patients studied is larger than that of CTV_0, see table 2. The relation between margin and average target volume for CTV_0 and ITV_n was fitted with the quadratic function of margin, as shown in figures 6 and 7. M_0 was then calculated based on these relations and the average volume of CTV_0 and ITV_n, as listed in table 2.

The relations between the margin and average OI_i for CTV_0 and ITV_n of low- and intermediate-risk prostate cancer patients are shown in figure 8. Without any margin added, the volume of ITV_n is larger than of CTV_0; therefore, the OI_i of ITV_n is larger than the OI_i of CTV_0. As the uniform margin increases, as expected, the OI_i approaches 1. The relation between margin and OI_i was fitted with the following function:

$$OI_i = 1 - \exp(P_0 \cdot \text{Margin} + P_1). \tag{5}$$

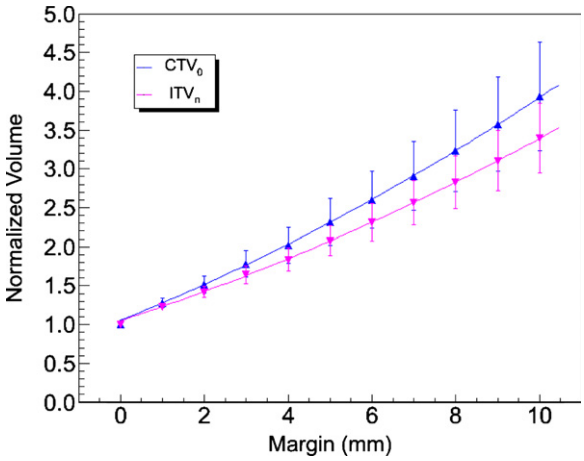

Figure 7. The relation between normalized target volume of CTV_0 and ITV_n versus the margin for intermediate-risk patients. The lines are fitted quadratic functions.

Table 2. The average volumes of CTV_0 and ITV_n. M_0 is the equivalent uniform margin for CTV_0 to have the equal volume as ITV_n.

Patient group	Vol(CTV_0) (cm^3)	Vol(ITV_n) (cm^3)	M_0 (mm)
Low risk	50.0 ± 20.4	61.2 ± 24.2	1.04 ± 0.58
Intermediate risk	67.9 ± 21.3	88.3 ± 25.3	1.24 ± 0.57

Table 3. The uniform margins needed to obtain an OI_i of 0.99 for CTV_0 and ITV_n, and the corresponding equivalent margin differences. Also given are the margin added volumes ($V_{0.99,CTV_0}$, $V_{0.99,ITV_n}$).

Patient group	$V_{0.99,CTV_0}$ (cm^3)	$V_{0.99,ITV_n}$ (cm^3)	$M_{C,0.99}$ (mm)	$M_{I,0.99}$ (mm)	ΔM (mm)
Low-risk patients	82.2 ± 36.2	66.8 ± 20.8	2.8 ± 0.9	0.4 ± 0.5	1.4 ± 0.8
Intermediate-risk patients	142.2 ± 53.1	104.0 ± 23.4	4.0 ± 1.6	0.8 ± 0.5	2.0 ± 1.0

The choice of function (5) is made because the normalized χ^2 (i.e. χ^2/ndf) of the fitting for both low-risk patient group ($\chi^2/\text{ndf} = 0.41$ for CTV_0 and 1.39 for ITV_n) and intermediate-risk patient group ($\chi^2/\text{ndf} = 0.44$ for CTV_0 and 1.22 for ITV_n) is close to 1.

The additional uniform margins ($M_{C,0.99}$ and $M_{I,0.99}$) required for CTV_0 or ITV_n to achieve 0.99 average OI_i were interpolated from the fitted relations (equation (5)), and further, the equivalent margin differences (ΔM) were calculated according to equation (4). The results are summarized in table 3.

4. Discussions and conclusions

In this study, geometric evaluation was performed for the hybrid strategy, and the benefit on margin reduction was compared to online image guidance only protocol. The margin in radiation therapy basically is a dosimetric concept (Langen and Jones 2001); therefore, dosimetric evaluation may be more important than the geometric study. However, the

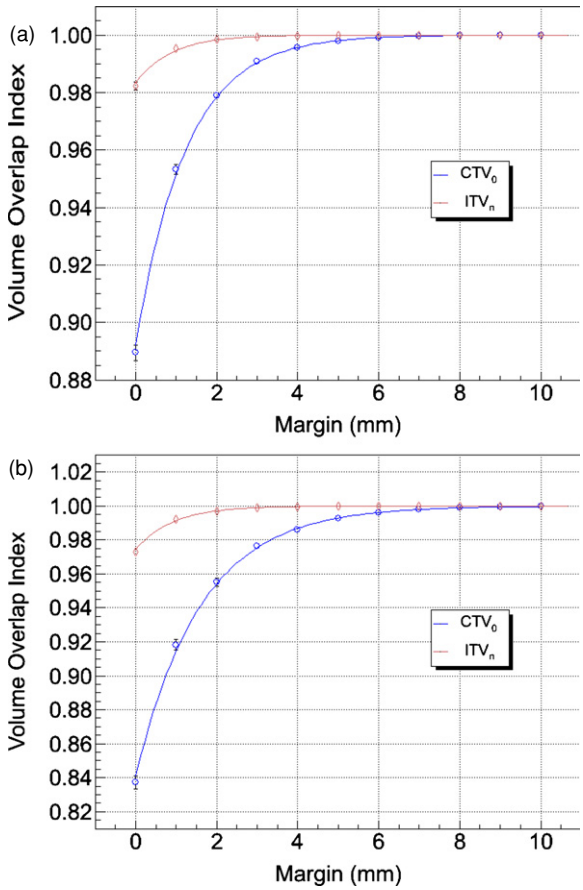

Figure 8. The fitted relations between the average volume overlap index (OI_i) and the corresponding margin added to CTV_0 and ITV_n, respectively, for (a) low-risk patients, (b) intermediate-risk patients.

dosimetric margin also depends on other factors such as the choice of photon energies, the beam arrangement and the modality of the treatment (3D conformal or IMRT). The detailed dosimetric evaluation is left for a future study. Nevertheless, the margin results we found in table 3 (M_C) are similar to the dosimetric margins for online IGRT alone found in a previous paper (Liang *et al* 2009).

Two image registration methods were used in different parts of this paper for online image guidance. A different cohort of patient data was used. In part 1 study, a group of patients treated under the online image guidance protocol was selected, in which CBCTs were available before and after each treatment fraction. The patients had gold markers (Visicoil) implanted in prostate gland which was used for online image guidance. In this study, the CTV is represented by the markers. In part 2 of the study, repeated helical CT (HCT) from patients undergoing regular treatment were selected; there are no implanted markers for this group of patients. Instead, CTV was delineated on CT images. The registration is made based on the center of mass (COM) of the CTV between treatment CT and planning CT to simulate the online image guidance.

The registrations of CTV for these two parts of the study are not exactly the same, even though the goal is the same, i.e. to align CTVs together. The marker-based registration should

be more accurate since that represents the CTV. The registration based on COM depends on the contours on treatment CT, which may have uncertainties. This was the reason that the helical CT was used for this part of the study because of its superior image quality to CBCT. Nevertheless, the uncertainties of contouring on CBCT under the offline image guidance environment have been discussed in a recent paper (Wang *et al* 2010). It was demonstrated that there were no significant differences in target volume definition between the methods using CBCT and helical CT for offline image guidance when multiple CBCTs were used for target volume delineation; the uncertainty is about 1–2 mm. Certainly this needs to be included in the clinical implementation of the hybrid strategy.

The accuracy of COM depends on the CTV definition. The CTV contours were delineated by a single experienced planner and were checked by others. The registration based on COM is simple to implement but may not be the most accurate ones. In a previous paper (Liang *et al* 2009), the COM registration was compared with the more accurate and robust normalized cross section methods and it was found that the results were very close when only translation correction was allowed.

We would like to point out that the movement of seminal vesicles (SV) is larger than the prostate for intermediate-risk group patients. However, the volume of the SV is also considerably smaller than prostate. Therefore, its contribution may not be as large as expected (Liang *et al* 2009). It is expected that the equivalent margins for intermediate-risk group should be larger than low-risk group patients; this was confirmed in table 3.

The margins determined in this study were uniform. However, because most of the prostate carcinoma occurs within the peripheral zone of the prostate (Chen *et al* 2000) and the rectal wall is directly posterior to the prostate, the posterior margin is critical. Studies have also shown that the inter-fractional prostate motion is greatest in anterior–posterior and superior–inferior directions, and least in the lateral directions (Rasch *et al* 2005). In addition, the SVs move independently from the prostate gland (Liang *et al* 2009) with larger magnitude. These suggest that the use of non-uniform margin may have some advantages in the prostate IGRT, with further reduced irradiated volume. This will be a subject of future study.

While the margin benefit may appear small in this study, 1.4 mm for low-risk patient group and 2.0 mm for intermediate-risk patient group, they should be considered in the context of image guidance. Our previous studies have shown that the online image guidance has greatly reduced the margin from over 10 mm to the order of 3–5 mm (Wu *et al* 2006; Liang *et al* 2009). These potential further margin reductions of 1–2 mm are based on the comparison with online image guidance alone with margins of 3–5 mm and are the benefit from adding the offline adaptive planning component. The margins cannot be zero because treatment uncertainties always exist, and further margin reduction studies are more difficult because many uncertainties need to be considered. Therefore, these margin reductions are significant improvements.

In conclusion, we have demonstrated that systematic inter-fractional prostate rotations exist, and they are patient specific. The rotations measured in before the treatment at each fraction, if not corrected, likely remained the same after the treatment. We also confirmed that the rotation distribution measured in the first five fractions is representative of those in the remaining treatment fractions. Therefore, the offline adaptive planning strategy is useful, even after online image guidance. Our simulation of the hybrid strategy of online image guidance and offline adaptive replanning can effectively account for the patient-specific inter-fractional organ motions and deformations. Compared with the online image guidance alone, the hybrid strategy can further reduce the margin by 1.4 mm for low-risk group patients and 2.0 mm for intermediate-risk group patients. Consequently, the target volume can be reduced by $(\Delta V/V)$

by 19% (15 cc) and 27% (38 cc), respectively. This should lead to a decreased dose to critical organs and treatment related complications.

Acknowledgments

This study is supported in part by grant CA118037 from the National Institute of Health. The contents are solely the responsibility of the authors and do not necessarily represent the official view of the NIH.

References

Amer A M, Mackay R I, Roberts S A, Hendry J H and Williams P C 2001 The required number of treatment imaging days for an effective off-line correction of systematic errors in conformal radiotherapy of prostate cancer—a radiobiological analysis *Radiother. Oncol.* **61** 143–50

Balter J M, Lam K L, Sandler H M, Littles J F, Bree R L and Ten Haken R K 1995a Automated localization of the prostate at the time of treatment using implanted radiopaque markers: technical feasibility *Int. J. Radiat. Oncol. Biol. Phys.* **33** 1281–6

Balter J M, Sandler H M, Lam K, Bree R L, Lichter A S and ten Haken R K 1995b Measurement of prostate movement over the course of routine radiotherapy using implanted markers *Int. J. Radiat. Oncol. Biol. Phys.* **31** 113–8

Bel A, Vos P H, Rodrigus P T, Creutzberg C L, Visser A G, Stroom J C and Lebesque J V 1996 High-precision prostate cancer irradiation by clinical application of an offline patient setup verification procedure, using portal imaging *Int. J. Radiat. Oncol. Biol. Phys.* **35** 321–32

Bos L J, van der Geer J, van Herk M, Mijnheer B J, Lebesque J V and Damen E M 2005 The sensitivity of dose distributions for organ motion and set-up uncertainties in prostate IMRT *Radiother. Oncol.* **76** 18–26

Chen M E, Johnston D A, Tang K, Babaian R J and Troncoso P 2000 Detailed mapping of prostate carcinoma foci: biopsy strategy implications *Cancer* **89** 1800–9

de Boer H C and Heijmen B J 2001 A protocol for the reduction of systematic patient setup errors with minimal portal imaging workload *Int. J. Radiat. Oncol. Biol. Phys.* **50** 1350–65

de Crevoisier R, Tucker S L, Dong L, Mohan R, Cheung R, Cox J D and Kuban D A 2005 Increased risk of biochemical and local failure in patients with distended rectum on the planning CT for prostate cancer radiotherapy *Int. J. Radiat. Oncol. Biol. Phys.* **62** 965–73

Ghilezan M J *et al* 2005 Prostate gland motion assessed with cine-magnetic resonance imaging (cine-MRI) *Int. J. Radiat. Oncol. Biol. Phys.* **62** 406–17

Heemsbergen W D, Hoogeman M S, Witte M G, Peeters S T, Incrocci L and Lebesque J V 2007 Increased risk of biochemical and clinical failure for prostate patients with a large rectum at radiotherapy planning: results from the Dutch trial of 68 GY versus 78 Gy *Int. J. Radiat. Oncol. Biol. Phys.* **67** 1418–24

Herman M G, Balter J M, Jaffray D A, McGee K P, Munro P, Shalev S, Van Herk M and Wong J W 2001 Clinical use of electronic portal imaging: report of AAPM Radiation Therapy Committee Task Group 58 *Med. Phys.* **28** 712–37

Koper P C, Heemsbergen W D, Hoogeman M S, Jansen P P, Hart G A, Wijnmaalen A J, van Os M, Boersma L J, Lebesque J V and Levendag P 2004 Impact of volume and location of irradiated rectum wall on rectal blood loss after radiotherapy of prostate cancer *Int. J. Radiat. Oncol. Biol. Phys.* **58** 1072–82

Langen K M and Jones D T 2001 Organ motion and its management *Int. J. Radiat. Oncol. Biol. Phys.* **50** 265–78

Liang J, Wu Q and Yan D 2009 The role of seminal vesicle motion in target margin assessment for online image-guided radiotherapy for prostate cancer *Int. J. Radiat. Oncol. Biol. Phys.* **73** 935–43

Millender L E, Aubin M, Pouliot J, Shinohara K and Roach M 3rd 2004 Daily electronic portal imaging for morbidly obese men undergoing radiotherapy for localized prostate cancer *Int. J. Radiat. Oncol. Biol. Phys.* **59** 6–10

Rasch C, Steenbakkers R and van Herk M 2005 Target definition in prostate, head, and neck *Semin. Radiat. Oncol.* **15** 136–45

Roeske J C, Forman J D, Mesina C F, He T, Pelizzari C A, Fontenla E, Vijayakumar S and Chen G T 1995 Evaluation of changes in the size and location of the prostate, seminal vesicles, bladder, and rectum during a course of external beam radiation therapy *Int. J. Radiat. Oncol. Biol. Phys.* **33** 1321–9

Stroom J C, Olofsen-van Acht M J, Quint S, Seven M, de Hoog M, Creutzberg C L, de Boer H C and Visser A G 2000 On-line set-up corrections during radiotherapy of patients with gynecologic tumors *Int. J. Radiat. Oncol. Biol. Phys.* **46** 499–506

Ten Haken R K, Forman J D, Heimburger D K, Gerhardsson A, McShan D L, Perez-Tamayo C, Schoeppel S L and Lichter A S 1991 Treatment planning issues related to prostate movement in response to differential filling of the rectum and bladder *Int. J. Radiat. Oncol. Biol. Phys.* **20** 1317–24

Van de Steene J, Van den Heuvel F, Bel A, Verellen D, De Mey J, Noppen M, De Beukeleer M and Storme G 1998 Electronic portal imaging with on-line correction of setup error in thoracic irradiation: clinical evaluation *Int. J. Radiat. Oncol. Biol. Phys.* **40** 967–76

Wang W, Wu Q and Yan D 2010 Quantitative evaluation of cone-beam computed tomography in target volume definition for offline image-guided radiation therapy of prostate cancer *Radiother. Oncol.* **94** 71–5

Wong J, Yan D, Michalski J, Graham M, Halverson K, Harms W and Purdy J 1995 The cumulative verification image analysis tool for offline evaluation of portal images *Int. J. Radiat. Oncol. Biol. Phys.* **33** 1301–10

Wu Q, Ivaldi G, Liang J, Lockman D, Yan D and Martinez A 2006 Geometric and dosimetric evaluations of an online image-guidance strategy for 3D-CRT of prostate cancer *Int. J. Radiat. Oncol. Biol. Phys.* **64** 1596–609

Yan D, Lockman D, Brabbins D, Tyburski L and Martinez A 2000 An off-line strategy for constructing a patient-specific planning target volume in adaptive treatment process for prostate cancer *Int. J. Radiat. Oncol. Biol. Phys.* **48** 289–302

Zelefsky M J, Fuks Z, Hunt M, Yamada Y, Marion C, Ling C C, Amols H, Venkatraman E S and Leibel S A 2002 High-dose intensity modulated radiation therapy for prostate cancer: early toxicity and biochemical outcome in 772 patients *Int. J. Radiat. Oncol. Biol. Phys.* **53** 1111–6